Developmental Biology 443 (2018) 1–9

Contents lists available at ScienceDirect

Developmental Biology

journal homepage: www.elsevier.com/locate/developmentalbiology

Lung morphogenesis is orchestrated through Grainyhead-like 2 (Grhl2) transcriptional programs

Ariena Kersbergen[a], Sarah A. Best[a,b], Sebastian Dworkin[c], Casey Ah-Cann[a,b], Michael E. de Vries[c,d], Marie-Liesse Asselin-Labat[a,b], Matthew E. Ritchie[e,f], Stephen M. Jane[d], Kate D. Sutherland[a,b,*]

[a] ACRF Stem Cells and Cancer Division, Walter and Eliza Hall Institute of Medical Research, Parkville, Victoria 3052, Australia
[b] Department of Medical Biology, The University of Melbourne, Parkville, Victoria 3010, Australia
[c] Department of Physiology, Anatomy and Microbiology, La Trobe University, Bundoora, Victoria 3086, Australia
[d] Department of Medicine, Monash University Central Clinical School, Prahran, Victoria 3004, Australia
[e] Molecular Medicine Division, Walter and Eliza Hall Institute of Medical Research, Parkville, Victoria 3052, Australia
[f] School of Mathematics and Statistics, The University of Melbourne, Parkville, Victoria 3010, Australia

ARTICLE INFO

Keywords:
Grhl2
Lung morphogenesis
Progenitor cells
Elf5

ABSTRACT

The highly conserved transcription factor Grainyhead-like 2 (Grhl2) exhibits a dynamic expression pattern in lung epithelium throughout embryonic development. Using a conditional gene targeting approach to delete *Grhl2* in the developing lung epithelium, our results demonstrate that Grhl2 plays multiple roles in lung morphogenesis that are essential for respiratory function. Loss of *Grhl2* leads to impaired ciliated cell differentiation and perturbed formation of terminal saccules. Critically, a substantial increase in Sox9-positive distal tip progenitor cells was observed following loss of *Grhl2*, suggesting that Grhl2 plays an important role in branching morphogenesis. Gene transcription profiling of *Grhl2*-deficient lung epithelial cells revealed a significant down regulation of *Elf5*, a member of the Ets family of transcription factors. Furthermore, ChIP and comparative genomic analyzes confirmed that *Elf5* is a direct transcriptional target of Grhl2. Taken together, these results support the hypothesis that Grhl2 controls normal lung morphogenesis by tightly regulating the activity of distal tip progenitor cells.

1. Introduction

Lung morphogenesis is under strict spatiotemporal control (Herriges and Morrisey, 2014; Warburton et al., 2000). During mouse embryogenesis, lung specification begins at embryonic day (E) 9.5 with the separation of the foregut into the future trachea and esophagus, and the formation of two primary lung buds. This is followed by a series of morphogenetic events involving crosstalk between the endoderm and mesoderm that ultimately gives rise to a complex branched network (Morrisey and Hogan, 2010; Short et al., 2013). In early lung development, distal tip epithelial cells marked by co-expression of Sox9 and Id2, function as multipotent progenitors giving rise to all mature lung epithelial cell types in two distinct developmental waves (Alanis et al., 2014; Rawlins et al., 2009). The bronchiolar lineage is specified first, triggered by the up regulation of Sox2, while cells exiting the tip downregulate Sox9 and co-express markers of alveolar type I (AT1) and alveolar type 2 (AT2) fate. As morphogenesis proceeds, these bipotent cells line the developing alveolar sacs and differentiate as mature AT1 or AT2 cells (Desai et al., 2014; Treutlein et al., 2014).

The Grainyhead-like (*Grhl*) gene family encodes highly conserved transcription factors remarkable for the functional diversity they display, with family members regulating numerous developmental processes including neural tube closure (Ting et al., 2003), epidermal barrier formation and wound healing (Caddy et al., 2010; Ting et al., 2005), brain morphogenesis and neural apoptosis (Dworkin et al., 2012) and craniofacial development (Dworkin et al., 2012, 2014). In humans, *GRHL2* is a clinically relevant gene in the context of lung diseases, whereby homozygous mutations in *GRHL2* have been linked with ectodermal dysplasia, deafness and hypodontia and critically bronchiolar asthma (Petrof et al., 2014). Alterations in the *GRHL2* gene have also been linked to bronchopulmonary dysplasia (BPD) (Wang et al., 2013), a chronic lung condition characterized by impaired alveolar development resulting in respiratory deficiency (Kinsella et al., 2006), and potential deregulation of maintenance of alveolar epithelial

* Correspondence to: Walter and Eliza Hall Institute of Medical Research, Parkville, Victoria 3052, Australia.
E-mail address: sutherland.k@wehi.edu.au (K.D. Sutherland).

https://doi.org/10.1016/j.ydbio.2018.09.002
Received 23 March 2018; Received in revised form 17 August 2018; Accepted 2 September 2018
Available online 05 September 2018
0012-1606/

integrity in idiopathic pulmonary fibrosis (Varma et al., 2014). Lastly, GRHL2 is implicated as an oncogene in the etiology and progression of non-small cell lung cancer (Dompe et al., 2011; Pan et al., 2017).

In the developing mouse lung, *Grhl2* exhibits the earliest, strongest and most persistent expression of the three *Grhl*-family members. *Grhl2* is expressed in the foregut endoderm at E10.5 and its expression progressively increases during branching morphogenesis (E12.5-E16.5). At E16.5, the tracheal epithelium and all epithelial cells lining the large and small bronchioles express high levels of *Grhl2* (Auden et al., 2006). After E16.5, *Grhl2* is dramatically down regulated, with low expression levels detected throughout the lung parenchyma as terminal differentiation commences. Consistent with these findings, in the human lung, *GRHL2* is expressed in both the luminal and basal cellular compartments of the small and large airways (Gao et al., 2013). Mice lacking *Grhl2* (*Grhl2*$^{-/-}$) exhibit embryonic lethality by E11.5 (Rifat et al., 2010), thus precluding the study of lung development past this stage. Interestingly, an N-ethyl-N-nitrosourea (ENU)-induced mutant *Grhl2* mouse survived, though exhibited defective lung morphogenesis (Pyrgaki et al., 2011). Enforced expression of dominant negative GRHL2 in primary human bronchial epithelial cells led to defects in cell morphogenesis, motility and adhesion (Gao et al., 2013). Loss of *Grhl2* in basal progenitor cells lining the pseudostratified airway epithelium had no effect on their self-renewal, there was reduced capacity of basal progenitor cells to differentiate along the ciliated cell lineage (Gao et al., 2015). However, no study to date has assessed the functional role of Grhl2 in lineage specification within the developing lung.

In this report, we utilized the well-characterized lung epithelial driver; *Shh-Cre* to conditionally delete *Grhl2* specifically in the developing lung of a novel *Grhl2*$^{f/f}$ mouse model. These mice enabled the investigation into the role of *Grhl2* in the initial establishment of the trachea and bronchial tree, as well as later roles for *Grhl2* in terminal cell specification. Loss of *Grhl2* function in lung epithelium resulted in death within hours of birth due to respiratory distress. Our results reveal unreported roles for Grhl2 in tracheal chondrogenesis and the regulation of distal lung progenitors, the latter of which is controlled through the direct regulation of *Elf5*, a novel Grhl2 target gene.

2. Results and discussion

2.1. Grhl2 deletion in the anterior foregut results in perinatal lethality

To overcome the embryonic lethality of *Grhl2* null mutants and address the function of Grhl2 in lung morphogenesis, we generated mice carrying a conditionally targetable *Grhl2* allele, with *loxP* sites flanking exon 2 (Fig. 1A). Mice homozygous for the floxed allele (*Grhl2*$^{f/f}$) were healthy and fertile, and when crossed with mice carrying a *B6-Cre* transgene, expressed at the two-cell stage of development, recapitulated the lethal phenotype of *Grhl2* null (*Grhl2*$^{-/-}$) mice (Rifat et al., 2010) (Fig. S1A). In line with this observation, analysis of *B6-Cre*;*Grhl2*$^{\Delta/-}$ embryos at E9.5, revealed a complete loss of *Grhl2* at the genomic level (Fig. S1B). To specifically delete *Grhl2* in lung epithelium, we crossed *Grhl2*$^{f/-}$ mice with *Shh-Cre* mice (Harfe et al., 2004), allowing us to excise *Grhl2* from the lung primordium from E9.5 (*Shh-Cre*;*Grhl2*$^{\Delta/-}$; hereafter *Grhl2*$^{\Delta/-}$). As the *Cre* allele was knocked into the *Shh* locus, resulting in loss of one *Shh* allele, *Shh-Cre*;*Grhl2*$^{\Delta/+}$ animals (hereafter *Grhl2*$^{\Delta/+}$) were used as controls. PCR analysis of genomic DNA isolated from epithelial (CD45$^-$CD31$^-$EpCAM$^+$) cells revealed efficient deletion of the *Grhl2* floxed allele specifically in lung epithelial cells of conditionally targeted mice (Fig. S1C). *Shh-Cre*-mediated deletion correlated with markedly reduced *Grhl2* mRNA expression and no evidence of compensatory up-regulation of *Grhl1* and *Grhl3* mRNA expression (Fig. 1B). Western blot analysis confirmed the absence of Grhl2 protein expression in *Grhl2*$^{\Delta/-}$ E16.5 lungs (Fig. 1C).

Until E18.5, *Grhl2*$^{\Delta/-}$ embryos were present at normal Mendelian ratios (Fig. 1D). Critically however, *Grhl2*$^{\Delta/-}$ newborns exhibited signs of respiratory distress and died within hours of birth, whereas *Grhl2* heterozygous (*Grhl2*$^{f/-}$ and *Grhl2*$^{\Delta/+}$) and wildtype (*Grhl2*$^{f/+}$) control mice were viable (Fig. 1D). In *Drosophila*, the antecedent member of the *Grhl* family, *grainyhead* (*grh*), contributes to tracheal organogenesis by regulating the size of the apical membrane and morphogenesis of tracheal epithelial cells (Hemphala et al., 2003). However, such a phenotype has yet to be ascribed to *Grhl* family members in mammals. Macroscopically, the tracheal tubes of *Grhl2*$^{\Delta/-}$ newborns appeared thinner and more fragile than littermate controls. Alcian blue staining of whole-mounted tracheas from post-natal day (PND) 0 *Grhl2* wildtype (wt; *Grhl2*$^{f/+}$) and heterozygous (het; *Grhl2*$^{f/-}$ and *Grhl2*$^{\Delta/+}$) control mice revealed uniform C-shaped cartilage rings (Fig. 1E). In contrast, tracheas from conditional knockout (null; *Grhl2*$^{\Delta/-}$) mice confirmed macroscopic observations and displayed severely disorganized cartilage rings (Fig. 1E). Tracheal stenosis was confirmed by measurement of tracheal width, which was significantly reduced in *Grhl2*$^{\Delta/-}$ mutants (Fig. 1F). No difference was observed in the length of the trachea (data not shown). Taken together, the abnormal formation of the tracheal rings and apparent tracheal stenosis likely contributes to the perinatal lethality of *Grhl2*$^{\Delta/-}$ mutant mice and underscores a non-cell autonomous function for Grhl2 in tracheal cartilage patterning.

2.2. Loss of Grhl2 results in perturbed lung morphogenesis

Histological analysis of lungs from *Grhl2*$^{\Delta/-}$ embryos at E18.5 revealed a disorganized architecture characterized by a reduction in distal saccules, thickened hypercellular intersaccular septa and a dense distribution of Nkx2.1-positive respiratory epithelial cells (Fig. 2A). Interestingly, total cell numbers (Fig. S2A) and the percentage of epithelial (CD31$^-$CD45$^-$EpCAM$^+$) cells (Fig. 2B) present in *Grhl2*$^{\Delta/-}$ mutant E18.5 lungs was comparable to that observed in *Grhl2*$^{\Delta/+}$ control lungs. Macroscopic analysis of *Grhl2*$^{\Delta/-}$ mutant lungs prior to birth, however, revealed a reduction in the size of the left lung lobe (Fig. S2B and C). Furthermore, quantification of distal airspace size, using T1-alpha as a marker of saccule boundaries (Fig. S2D), revealed a significant reduction in the saccule size in *Grhl2*$^{\Delta/-}$ E18.5 lungs (Fig. 2C) when compared to *Grhl2*$^{\Delta/+}$ littermate controls. Taken together, *Grhl2* loss results in a condensed cellular morphology, due to a reduction in lung size.

To explore whether *Grhl2* loss effected branching morphogenesis, we employed the mouse embryonic lung culture assay system (Warburton et al., 1992) and compared the growth of *Grhl2* wildtype (wt; *Grhl2*$^{f/+}$), heterozygous (het; *Grhl2*$^{f/-}$, *Grhl2*$^{\Delta/+}$) and conditional knockout (null; *Grhl2*$^{\Delta/-}$) E11.5 lungs cultured *ex vivo* for 72 h. Interestingly, *Grhl2* heterozygous and knockout lungs exhibited significantly more airway tips (Fig. 2D and E), a direct readout of branch number, suggesting that reduced Grhl2 expression results in increased branching morphogenesis. Grhl family members have been implicated in the control of cytoskeletal dynamics, with Grhl2 involved in the regulation of the epithelial apical junctional complex through its ability to directly modulate expression of *E-cadherin* and *Claudin 4* (Werth et al., 2010). Given that proper epithelial cell arrangement is crucial for branching morphogenesis, we assessed Claudin 4 (*Cldn4*) transcript levels in whole lung tissue isolated from E16.5 *Grhl2*$^{\Delta/+}$ and *Grhl2*$^{\Delta/-}$ embryos. Interestingly, *Cldn4* mRNA expression was significantly down regulated in the absence of *Grhl2* (Fig. 2F). Notably, immunofluorescence staining revealed the maintenance of Claudin 4 expression in epithelial cells lining the proximal airways of *Grhl2*$^{\Delta/-}$ E16.5 lungs (Fig. S2E), but a complete absence of expression in distal epithelium (Fig. 2G). Expression of β-catenin was maintained in both the proximal and distal airway compartments (Fig. S2E and Fig. 2G). The correct formation of adherence junctions in the absence of Grhl2 was further confirmed by no change in E-cadherin expression at both the mRNA (Fig. 2F) and protein (Fig. S2F) levels, suggesting that alternate

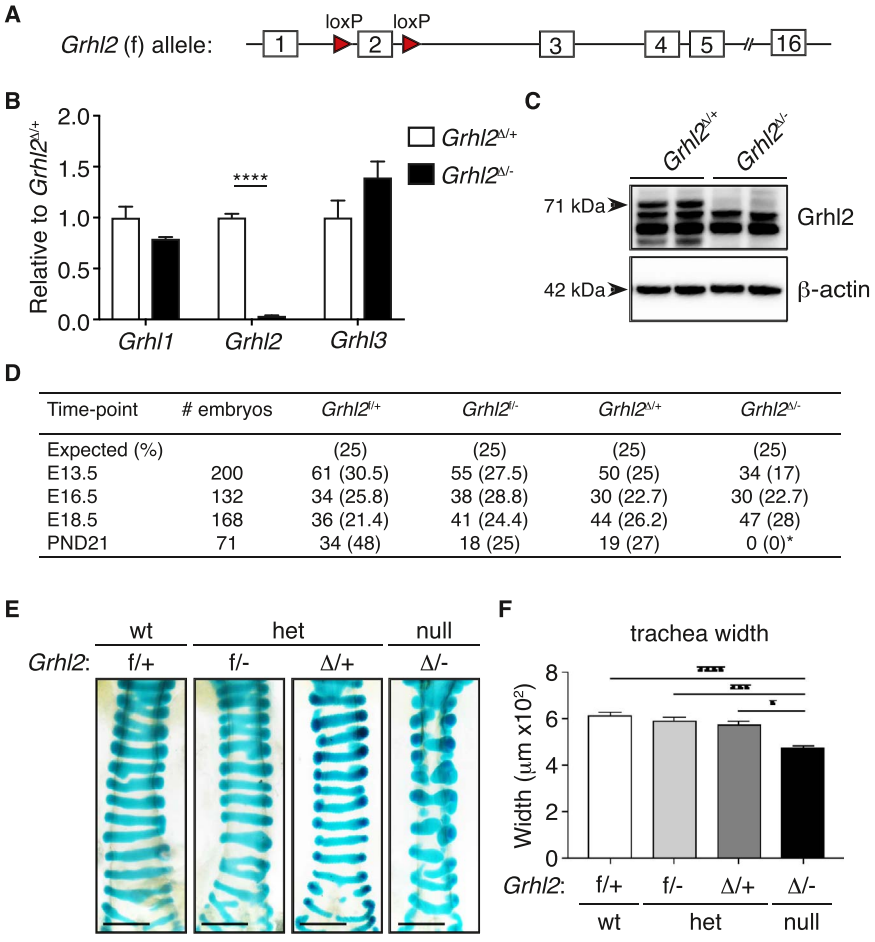

D

Time-point	# embryos	*Grhl2*$^{f/+}$	*Grhl2*$^{f/-}$	*Grhl2*$^{Δ/+}$	*Grhl2*$^{Δ/-}$
Expected (%)		(25)	(25)	(25)	(25)
E13.5	200	61 (30.5)	55 (27.5)	50 (25)	34 (17)
E16.5	132	34 (25.8)	38 (28.8)	30 (22.7)	30 (22.7)
E18.5	168	36 (21.4)	41 (24.4)	44 (26.2)	47 (28)
PND21	71	34 (48)	18 (25)	19 (27)	0 (0)*

Fig. 1. Loss of *Grhl2* in lung epithelium results in perinatal lethality. (A) Schematic representation of the *Grhl2* conditional (f) allele. *LoxP* sites flank exon 2 of the *Grhl2* gene. (B) Quantitative RT-PCR analysis of *Grhl1*, *Grhl2* and *Grhl3* mRNA expression in whole lung tissue isolated from E16.5 *Grhl2*$^{Δ/-}$ embryos relative to *Grhl2*$^{Δ/+}$ lung tissue (n = 3 per genotype). Mean ± SEM. ****p < 0.0001. (C) Western blot analysis of Grhl2 in protein lysates prepared from E16.5 control and *Grhl2*$^{Δ/-}$ lungs (n = 2 embryos). β-actin provides the protein loading control. (D) Ratios of genotypes observed in litters of crosses between *Shh-Cre*;*Grhl2*$^{Δ/-}$ and *Grhl2*$^{f/f}$ mice. The observed percentage is shown in parentheses. $^{*}\chi^2$ was used to compare expected and observed number of offspring. ****p < 0.0001. (E) Whole-mount Alcian Blue staining of *Grhl2* wildtype (wt; *Grhl2*$^{f/+}$), heterozygous (het; *Grhl2*$^{f/-}$, *Grhl2*$^{Δ/+}$) and conditional knockout (null; *Grhl2*$^{Δ/-}$) tracheas at birth. Scale, 500 μm. (F) Quantification of tracheal width in *Grhl2* wildtype (wt; *Grhl2*$^{f/+}$, n = 11), heterozygous (het; *Grhl2*$^{f/-}$, n = 11, *Grhl2*$^{Δ/+}$, n = 6) and conditional knockout (null; *Grhl2*$^{Δ/-}$, n = 19) post-natal day 0 (PND0) mice. Mean ± SEM. *p = 0.0286; ***p0.0002; ****p < 0.0001.

pathways maintain E-cadherin expression in lung epithelium. As mice lacking *Cldn4* are viable, and display only minor physiological lung impairment (Kage et al., 2014), reduced Claudin 4 cannot therefore account for all the morphological defects observed in *Grhl2*$^{Δ/-}$ lungs. Thus, other critical Grhl2 targets likely direct the morphogenesis and integrity of lung epithelium.

2.3. Impaired epithelial differentiation following loss of Grhl2

Recent studies have revealed the importance of Grhl2 in the differentiation of basal progenitor cells along the ciliated cell lineage (Gao et al., 2015). To address whether Grhl2 is also crucial for the differentiation of proximal progenitor cells we first examined the expression of Sox2, a transcription factor required for the generation of mature secretory and ciliated cell lineages of the conducting airways (Gontan et al., 2008; Que et al., 2009; Tompkins et al., 2011). Immunohistochemical staining revealed no significant changes in Sox2 expression at E18.5 (Fig. 3A and B), suggesting that airway precursor cells develop normally in the absence of *Grhl2*. Moreover, no apparent change in expression of CC10-positive club cells (Fig. 3C and D), and secretoglobin 3a2 (Scgb3a2) (data not shown), a marker of club cell precursors, was observed in *Grhl2*$^{Δ/-}$ lungs. Notably, a reduction in the number of ciliated cells, as assessed by FoxJ1 (Fig. 3E and F) staining was observed in *Grhl2*$^{Δ/-}$ mutant lungs. This observation is in line with recently published findings in tracheal epithelium (Gao et al., 2015), and independently confirms a critical role for Grhl2 in controlling ciliated cell differentiation.

To determine whether distal progenitor development was disrupted in *Grhl2*$^{Δ/-}$ mutant lungs, we examined the expression of Sox9, a marker of distal progenitor cells, whose expression is down regulated by E18.5 as differentiation of the alveolar lineage progresses (Rockich et al., 2013). Interestingly, Sox9-expressing cells were still detected in *Grhl2*$^{Δ/-}$ mutant lungs when these cells were markedly reduced in *Grhl2*$^{Δ/+}$ control lungs at E18.5 (Fig. 3G and H; Fig. S3A). These results are consistent with a delay in the differentiation of Sox9-positive precursor cells, or augmented branching morphogenesis. To analyze distal epithelial cell differentiation in greater detail in *Grhl2*$^{Δ/-}$ mutant lungs, we performed immunostaining with antibodies specific for alveolar type II (pro-SPC) and type I (T1α) cells. While the distribution of pro-SPC-positive AT2 cells was dense in *Grhl2*$^{Δ/-}$ lungs (Fig. 3I and J), quantification of pro-SPC^{+} nuclei revealed a reduction in the number of pro-SPC-expressing cells following loss of *Grhl2* (Fig. S3B). No apparent change in the expression of AT1 (T1α) cells was detected in *Grhl2*$^{Δ/-}$ lungs (Fig. 3K and L). To assess whether *Grhl2*$^{Δ/-}$ mutant epithelial cells exhibit enhanced progenitor cell activity, we isolated EpCAM^{+} cells from *Grhl2*$^{Δ/-}$ and *Grhl2*$^{Δ/+}$ control E16.5 lungs. The E16.5 time-point was chosen to enrich for Sox9-expressing distal progenitor cells, while allowing us to obtain sufficient cell numbers from individual lungs for *in vitro* colony assays. Sorted EpCAM^{+} cells were then embedded on a Matrigel base layer and assayed for colony

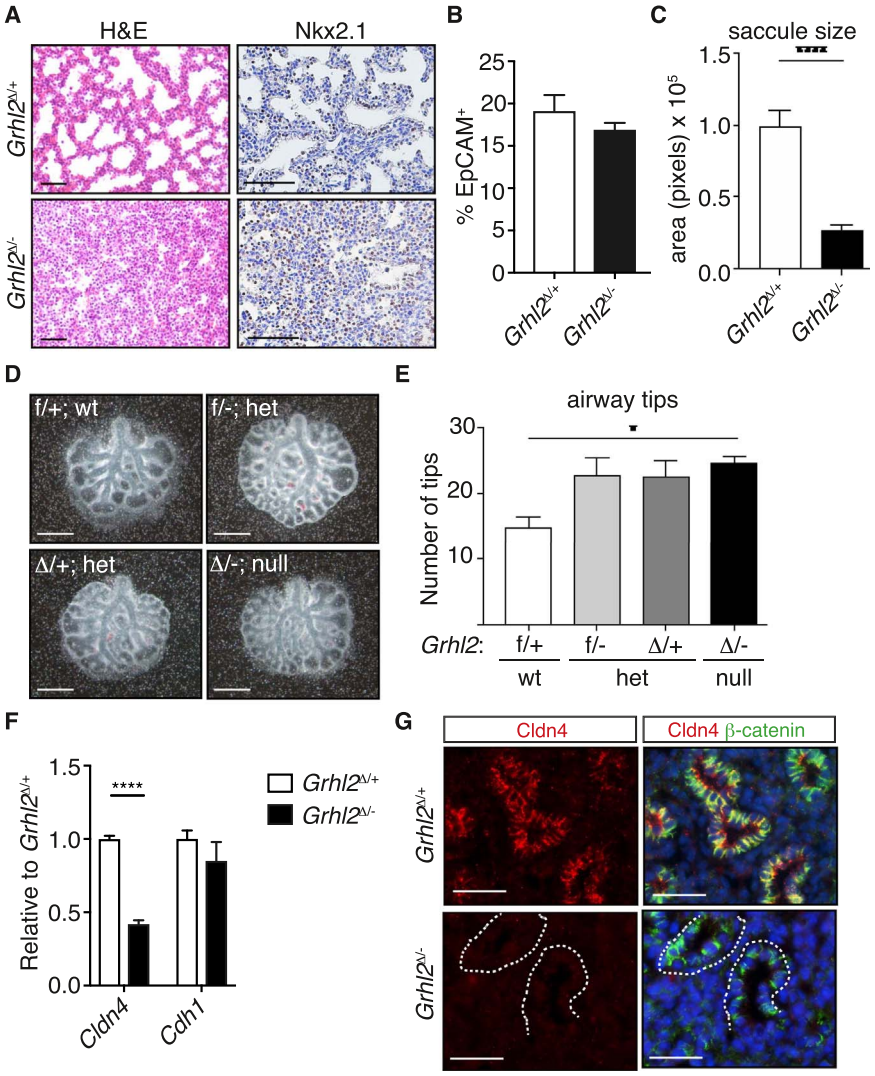

Fig. 2. Loss of *Grhl2* expression in lung epithelium results in perturbed lung morphogenesis. (A) Representative H & E and Nkx2.1 immunostaining of lungs from E18.5 $Grhl2^{\Delta/+}$ control and $Grhl2^{\Delta/-}$ mutant embryos. Scale, 100 μm. (B) Percentage $CD31^{-}CD45^{-}EpCAM^{+}$ cells in $Grhl2^{\Delta/+}$ control (n = 10) and $Grhl2^{\Delta/-}$ mutant (n = 7) E18.5 lungs. Mean ± SEM. (C) Quantification of saccule size in $Grhl2^{\Delta/+}$ control (n = 5) and $Grhl2^{\Delta/-}$ mutant (n = 6) E18.5 lungs. Mean ± SEM. ****p < 0.0001. (D) Representative images of E11.5 *Grhl2* wildtype (wt; $Grhl2^{f/+}$), heterozygous (het; $Grhl2^{f/-}$, and $Grhl2^{\Delta/+}$) and conditional knockout (null; $Grhl2^{\Delta/-}$) lungs following 72 h of *ex vivo* culture. Scale, 0.5 mm. (E) Quantification of airway tips in *Grhl2* wildtype (wt; $Grhl2^{f/+}$, n = 6), heterozygous (het; $Grhl2^{f/-}$, n = 4, $Grhl2^{\Delta/+}$, n = 7) and conditional knockout (null; $Grhl2^{\Delta/-}$, n = 7). Mean ± SEM. *p = 0.0156. (F) Quantitative RT-PCR analysis of *Cdh1* and *Cldn4* mRNA expression in whole lung tissue isolated from E16.5 $Grhl2^{\Delta/-}$ embryos relative to control lung tissue (n = 3 per genotype). Mean ± SEM. ****p < 0.0001. (G) Representative immunofluorescence co-staining of Claudin-4 (Cldn4; red) with β-catenin (green) on $Grhl2^{\Delta/+}$ control and $Grhl2^{\Delta/-}$ mutant E16.5 lungs. Scale, 30 μm.

formation on day 14 (Fig. S3C). Similar to colonies derived from the distal lung epithelium (Bilodeau et al., 2014), colonies that grew were small with irregular morphologies (Fig. S3D). Critically however, the colony formation potential of $Grhl2^{\Delta/-}$ mutant epithelial cells was significantly higher than seen with $Grhl2^{\Delta/+}$ control epithelium (Fig. S3E). Taken together, these findings suggest that Grhl2 regulates the activity of Sox9-expressing progenitor cells in the distal compartment of the developing lung and effects their ability to differentiate along the AT2 cell lineage.

2.4. *Elf5 is a novel target of Grhl2 in lung epithelium*

To identify direct transcriptional targets responsible for the observed increase in distal progenitor cells in $Grhl2^{\Delta/-}$ lungs, we performed RNA-seq on epithelial ($EpCAM^{+}$) cells from $Grhl2^{\Delta/-}$ mutant and control E16.5 lungs. Statistical analysis using the limma software (Ritchie et al., 2015) identified gene expression changes in $Grhl2^{\Delta/-}$ epithelium with 353 down regulated genes (blue; FDR < 0.05), and 277 up regulated genes (red; FDR < 0.05) (Fig. 4A; Table S1). In line with the observed defect in differentiation along the ciliated cell lineage following loss of *Grhl2* (Fig. 3A) (Gao et al., 2015), gene ontology (GO) analysis revealed a significant underrepresentation of genes implicated in cilia development (Fig. S4A). Notch signalling is critical in controlling the balance between ciliated cells and secretory cells during lung morphogenesis (Gao et al., 2015; Guseh et al., 2009; Tsao et al., 2009). However, in contrast to previous studies (Gao et al., 2015; Guseh et al., 2009; Tsao et al., 2009), KEGG pathway analysis failed to reveal changes in Notch pathway components, including *Notch1*, *Notch3*, *Jag1* and *Jag2* genes (Fig. S4B), which are putative direct Grhl2 targets based on promoter occupancy by Grhl2 in chromatin immunoprecipitation (ChIP)-seq analyses (Gao et al., 2015). These data suggest that Grhl2 does not function upstream of the Notch pathway, however, expression of transcription factors known to promote ciliogenesis; *Multicilin* (*Mcidas*), and *Znf750*, the latter a recently described Grhl2 target in the regulation of ciliogenesis (Gao et al., 2015), were both significantly down regulated in $Grhl2^{\Delta/-}$ epithelium (Fig. S4C). This confirms the integral role for Grhl2 in ciligogenesis in the developing lung.

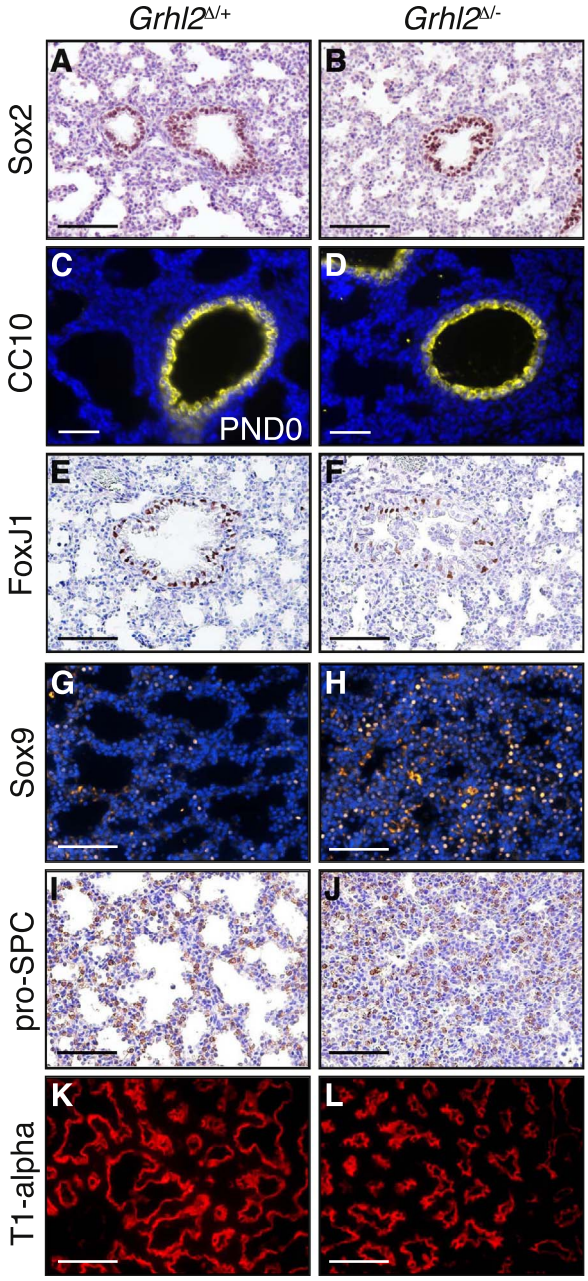

Fig. 3. *Grhl2* loss results in defective epithelial differentiation. Representative immunohistochemical staining of sections from $Grhl2^{\Delta/+}$ control and $Grhl2^{\Delta/-}$ lungs for (A, B) Sox2, (C, D) CC10, (E, F) FoxJ1, (G, H) Sox9, (I, J) pro-SPC and (K, L) T1-alpha protein expression. Representative images of E18.5 lungs are shown for Sox2, FoxJ1, Sox9, pro-SPC, T1-alpha and of PND0 lungs for CC10. Scale, 50 μm.

Elf5, a member of the Ets family of transcription factors, plays important roles in epithelial fate decisions (Oakes et al., 2008). Elf5 is expressed in differentiating keratinocytes and branching epithelia such as the salivary gland, prostate, mammary gland and kidney (Oettgen et al., 1999; Zhou et al., 1998). In the developing mouse lung, Elf5 expression exhibits a dynamic expression pattern. In early development Elf5 expression is restricted to distal epithelium, and from the end of gestation, expression is enriched in proximal epithelial cells and lost in distal epithelium (Metzger et al., 2008, 2007). Moreover, expression of *ELF5* was recently demonstrated to be among a set of transcription factors enriched in human epithelial tip progenitors (Nikolic et al., 2017). Interestingly, Elf5 was strongly down regulated in $Grhl2^{\Delta/-}$ mutant epithelium (Fig. 4A, FDR < 0.05). Consistent with this finding, we confirmed a marked reduction in Elf5 expression in the developing lungs of $Grhl2^{\Delta/-}$ mutant embryos at both the mRNA (Fig. 4B) and protein level (Fig. 4C).

The *Grhl* DNA consensus-binding site (5'-AACCGGTT-3') is highly conserved across species (Ting et al., 2005), and recent genome-wide ChIP studies have revealed an enrichment of GRHL2 ChIP peaks at transcriptional start sites, promoters and within intronic regions (Aue et al., 2015; Gao et al., 2013; Walentin et al., 2015). Utilizing an *in silico* approach, we interrogated the 630 differentially expressed genes (Fig. 4A), for the presence of a *Grhl* binding site (Jolma et al., 2013) 5 kb upstream of transcriptional start sites, and inside gene bodies. This approach revealed the presence of two putative Grainyhead consensus motifs within an intronic region of the *Elf5* gene (Fig. 4D), of which site 1 is highly conserved (Fig. 4D). These findings suggest that Grhl2 may regulate *Elf5* expression in lung epithelial cells. To test this observation, we performed ChIP on whole embryonic lungs, or purified mesenchymal ($EpCAM^-$) cells as a control for cells in which Grhl2 is not expressed (Auden et al., 2006). We confirmed specific binding of Grhl2 to site 1 of *Elf5* (Fig. 4E and Fig. S5), and to two sites in *Cldn4*, a bona fide Grhl2 target (Fig. S5). Overexpression of Elf5 in the embryonic lung disrupts branching morphogenesis and leads to a block in alveolar and airway differentiation (Metzger et al., 2008). To explore whether Grhl2 regulates distal progenitor cells through the activation of Elf5, we compared the expression of differentially expressed genes in $Grhl2^{\Delta/-}$ epithelium with the gene signature of E16.5 *SFTPC/Elf5* lungs derived from Metzger et al. (2008). Gene set testing revealed a statistically significant enrichment for Elf5 signature genes among the genes down regulated in the absence of *Grhl2* (Fig. 4F, P = 0.0085). These findings provide additional evidence that *Elf5* is a direct Grhl2 target, crucial in regulating the differentiation of distal lung epithelium.

In conclusion, our results present new evidence for a crucial role of Grhl2 in respiratory function. In the embryonic trachea, Grhl2 plays a non-cell autonomous role in the differentiation of tracheal mesenchyme (Fig. S6). In future studies it will be important to determine whether restricted loss of *Grhl2* in the tracheal epithelium disrupts paracrine signalling cascades from the epithelium to the underlying mesenchyme or directly regulates the expression of transcription factors, such as Sox2 (Que et al., 2009), crucial for tracheal cartilage patterning. In the proximal airways, consistent with previous studies (Gao et al., 2015), conditional deletion of *Grhl2* leads to a reduction in the number of ciliated cells (Fig. S6), reinforcing the importance of Grhl2 in ciliogenesis. In the distal compartment, the number of Sox9-positive progenitor cells is increased in the absence of *Grhl2* (Fig. S6), likely the result of augmented branching morphogenesis. Importantly, we describe a novel transcriptional axis between Grhl2 and Elf5, an interaction which likely influences the activity of distal tip progenitor cells and may be a key network in lung homeostasis.

3. Materials and methods

3.1. Generation of experimental animals

All animal experiments were conducted according to the Walter and Eliza Hall Institute of Medical Research Animal Ethics Committee guidelines (AEC 2013.028, 2016.024) or approved by the AMREP Animal Ethics Committee. The generation and genotyping of $Grhl2^{+/-}$ mice have been described previously (Rifat et al., 2010). B6-*Cre* (Schwenk et al., 1995) and *Shh-Cre* (Harfe et al., 2004) mice were obtained from Jackson Laboratories. The construction and validation of the *Grhl2* targeting vector will be described elsewhere and genotyped using the primer set outlined in Table S2. $Grhl2^{+/-}$ mice were crossed with *Shh-Cre* mice, and the resultant animals were crossed with $Grhl2^{f/f}$ mice to produce *Shh-Cre*;$Grhl2^{\Delta/-}$ ($Grhl2^{\Delta/-}$) experimental mice, where Δ is the deleted floxed allele. *Shh-Cre*;$Grhl2^{\Delta/+}$ ($Grhl2^{\Delta/+}$) mice were used as controls.

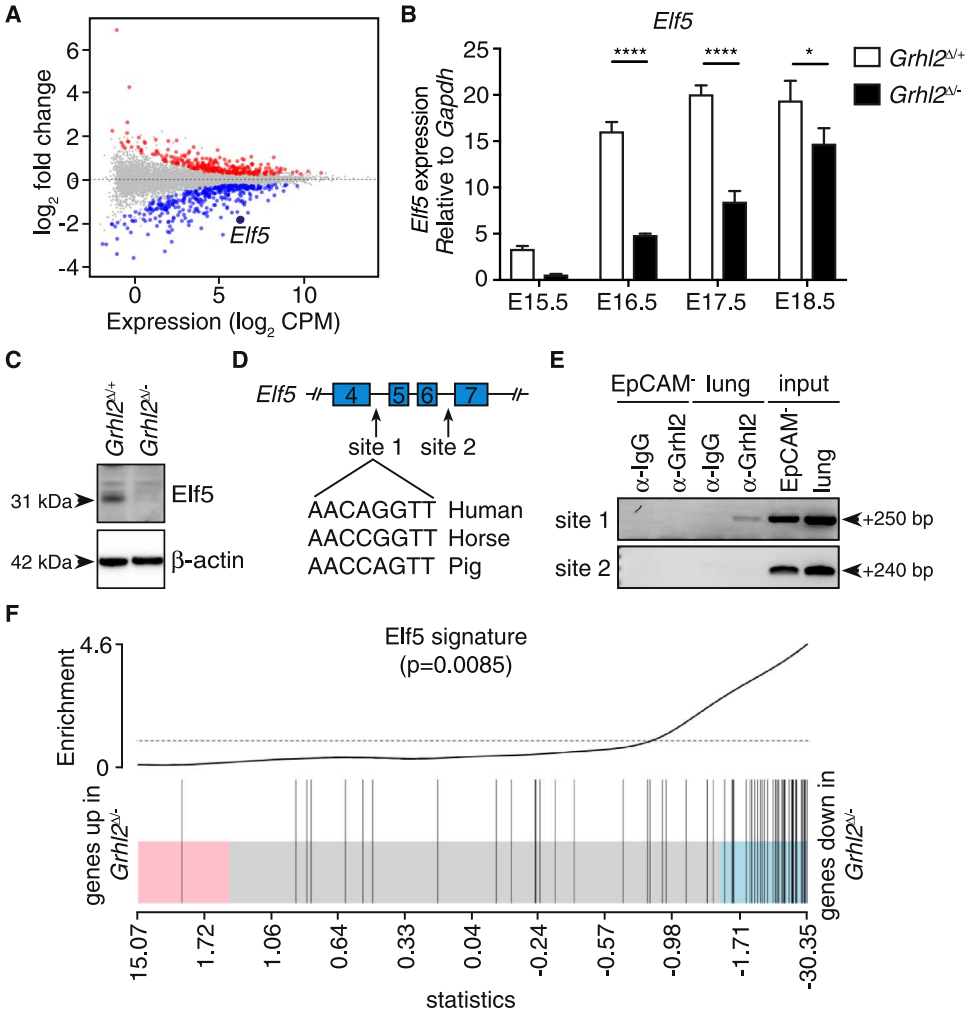

Fig. 4. *Elf5* is a direct transcriptional target of Grhl2 in lung epithelium. (**A**) A plot of differentially expressed genes (up-regulated in red; down-regulated in blue) between *Grhl2*$^{\Delta/-}$ mutant and *Grhl2*$^{\Delta/+}$ control EpCAM^{+} epithelial cells isolated from E16.5 embryonic lungs. (**B**) Quantitative RT-PCR analysis of *Elf5* mRNA levels in whole lungs at E15.5, E16.5, E17.5 and E18.5 (n = 3 per time point). Mean ± SEM. *p = 0.0461, ****p < 0.0001. (**C**) Western blot analysis of Elf5 in E16.5 control and *Grhl2*$^{\Delta/-}$ lungs. β-actin provided the protein loading control. (**D**) Schematic of conserved Grhl2 consensus site in intron 4/6 of the *Elf5* gene. (**E**) ChIP in E16.5 whole lungs and mesenchymal (EpCAM^{-}) cells sorted from E16.5 C57BL/6 lungs served as a negative control. ChIP was performed with a Grhl2 antibody or an immunoglobulin G (IgG; negative control) antibody. (**F**) Gene set analysis of differentially expressed genes in *Grhl2*$^{\Delta/-}$ mutant epithelium compared to the alveolar type II signature genes from mice engineered to overexpress Elf5 in lung epithelium (Metzger et al., 2008) (*roast* gene set test p < 0.0005). Index marks indicate genes from the Alveolar type II/Elf5 signature. (For interpretation of the references to color in this figure legend, the reader is referred to the web version of this article).

3.2. Histology and Immunohistochemistry

For histological analysis, lungs were fixed in 4% paraformaldehyde in phosphate-buffered saline (PBS), embedded in paraffin and sections (2 μm) prepared and stained by Haematoxylin and Eosin (H & E). Alternatively, following fixation, lungs were embedded in 7.5% gelatin, 15% sucrose and snap frozen for the preparation of frozen tissue sections (10 μm). For immunohistochemistry, sections were blocked in 10% serum prior to incubation with specific antibodies, followed by biotin-conjugated secondary antibodies (Table S3). For mouse primary antibodies, the Mouse on Mouse (M.O.M™) Kit (Vector Laboratories BMK-2202) and the Streptavidin/Biotin Blocking Kit (Vector Laboratories SP-2002), were used according to the manufacturer's instructions. Signal was amplified using Vectorstain Elite ABC HRP Kit (Vector Laboratories PK-6100) for 30 min, followed by 3, 3'-diaminobenzidine (DAKO K3468). Sections were counterstained with Haematoxylin.

For immunofluorescence staining, sections were blocked in 10% serum, incubated with appropriate antibodies overnight at 4 °C followed by fluorophore-conjugated antibodies (Table S3). Slides were imaged on the Zeiss AxioObserver microscope using Zen software (Zeiss). Quantification of Sox9 and pro-SPC staining was automated through custom-written ImageJ Macros (using the FIJI distribution package) (Schindelin et al., 2012). Segmentation was performed using the color deconvolution plug-in, filtering and defined thresholds on each of the stains.

For wholemount alcian blue staining, dissected postnatal day 0 (PND0) tracheas were fixed in 95% ethanol for 12 h followed by overnight staining with 0.03% alcian blue dissolved in 80% ethanol and 20% acetic acid.

3.3. Flow cytometry

Individual lungs (E16.5 or E18.5) were digested in 2 mg/mL Collagenase I (Worthington LS004197) in 0.2 g/L DPBS/glucose for 30 min at 37 °C and red blood cells were lysed in 0.8% NH_4Cl (Sigma A4514) for 3 min at RT. Samples were blocked in FcR blocking reagent (Milteny Biotech 130-092-575) in 0.1 mg/mL Rat IgG for 10 min at 4 °C. Primary antibodies (Table S3) were incubated for 30 min at 4 °C, as previously described (Galvis et al., 2015). Flow cytometry was performed using an ARIA sorter (Beckton Dickinson) and analyzed using FlowJo software (FlowJo LLC).

3.4. In vitro colony assay

Freshly sorted CD45$^-$CD31$^-$EpCAM$^+$ epithelial cells were resuspended in DMEM/F-12 + Glutamax, supplemented with B27 Supplement (Gibco 17504044), insulin-transferrin-sodium selenite (ITS) Supplement (Gibco 41400045), Heparin, 20 ng/mL fibroblast growth factor (FGF) and 10 ng/mL epidermal growth factor (EGF). Cells at a density of 7500 cells/200 µl were seeded on top of a cushion of 50% growth factor reduced Matrigel (BD Biosciences) in DMEM/F-12 + Glutamax. Cells were cultured in a low oxygen incubator for 14 days, with media changes every other day. Seven independent litters were used in experiments with each experiment containing at least one *Grhl2*$^{\Delta/+}$ and one *Grhl2*$^{\Delta/-}$ embryo. Colonies were imaged and scored using ImageJ software (Schindelin et al., 2012).

3.5. Ex vivo lung culture

E11.5 lungs were isolated and cultured in an air-liquid interface on an 8 µm membrane placed on 1 mL of DMEM/F-12 + Glutamax, supplemented with 100 U/mL penicillin and 100 µg/mL streptomycin.

3.6. RNA isolation and quantitative RT-PCR

RNA was isolated from embryonic lung tissue using TRIzol™ (Thermo Scientific 15596026) or the miRNeasy Mini Kit (Qiagen 74106) according to the manufacturer's specifications. DNase treatment was performed using TURBO™ DNA-free Kit (Ambion AM1907). cDNA was synthesized using the Superscript III kit (Thermo Scientific 18080051). Quantitative RT-PCR was performed using the SensiMix™ SYBR® Hi-ROX kit (Bioline QT605-05) on the Viia7 Real-Time PCR System (Thermo Scientific) with primers (Table S2). Relative mRNA was calculated compared to *Gapdh* internal control using the delta-delta-cT statistical method.

3.7. RNA-seq and genome-wide motif analysis

Reads were aligned to the *Mus musculus* genome (mm10) using the Rsubread package (Liao et al., 2013) and assigned to genes by the featureCounts function (Liao et al., 2014) using the in-built RefSeq annotation. Filtering and normalization used the edgeR package (Robinson et al., 2010). Genes with low expression (defined as having a count per million (CPM) of less than 0.5 in fewer than 3 samples) were removed from further analysis. Compositional differences between libraries were normalized using the trimmed mean of *M*-values (TMM) method (Robinson and Oshlack, 2010). Subsequent differential expression analysis was performed using the limma package (Ritchie et al., 2015). Counts were transformed to log2-CPM values (with an offset of 0.5) with associated observational and sample-specific weights obtained from the voomWithQualityWeights method (Liu et al., 2015) assuming a linear model with effects for genotype, sex and a blocking effect for littermates. Contrasts between the different groups; *Grhl2*$^{\Delta/-}$ (epithelial; EpCAM$^+$) versus *Grhl2*$^{\Delta/+}$ (epithelial; EpCAM$^+$), were estimated and differential expression was assessed using moderated *t*-statistics. Genes were ranked according to their false discovery rate (FDR), and those with FDR < 0.05 were considered differentially expressed. Gene ontology analysis used the *goana* function, which includes a correction for gene length bias as per *goseq* (Young et al., 2010) and KEGG analysis used the *kegga* function, both from limma. Gene set testing using the *roast* method (Wu et al., 2010) was applied on the Metzger *et al.* (Metzger et al., 2008) alveolar type II gene expression signatures. The data is available from GEO (Accession Number GSE105781).

The *Mus musculus* (mm10) genome was scanned for Grhl2 motifs obtained from Jolma *et al.* (Jolma et al., 2013) using FIMO (Grant et al., 2011) and assigned to genes using the ChIPpeakAnno package (Zhu et al., 2010) when they occurred within a 5kB window upstream of the promoter or inside the gene body (setting *upstream & inside* in annotatePeakInBatch).

3.8. ChIP and Western blot analyses

ChIP was performed on E16.5 C57BL/6 lung cells as previously described (Merino et al., 2015; Voss et al., 2012), with anti-GRHL2 (Sigma HPA004820) and rabbit anti-IgG (Cell Signalling 3900 S). Freshly isolated CD31$^-$CD45$^-$EpCAM$^-$ cells were used as a negative control. Shearing was performed to generate fragments approximately 500 bp in size. PCR primers used are listed in Table S2.

Protein lysates from mouse lung tissue were prepared in KALB lysis buffer (150 mM NaCL; 1 mM EDTA; 50 mM Tris. HCl, pH 7.5; 10 mM NaF; 1 mM Na_3VO_4; 1 mM PMSF; 1% Triton X-100) containing cOmplete Protease Inhibitor Cocktail (Roche 11697498001) as previously described (Barker et al., 2008).

3.9. Statistics

Statistical analysis was performed using GraphPad Prism software (GraphPad Software). Pairwise comparisons were performed using an unpaired Student *t*-test and multivariate comparisons were performed using one-way ANOVA (Kruskal-Wallis test) with Tukey's multiple comparisons test or two-way ANOVA with Dunn's multiple comparisons test for grouped analyses. For qRT-PCR studies, Gaussian distribution was applied.

Acknowledgements

We are grateful to L. Scott, H. Johnson and K. Birchall for animal husbandry, E. Tsui and C. Tsui in the WEHI Histology Facility for expert support, L. Whitehead and K. Rodger in the WEHI Imaging Facility for imaging support and assistance with the quantification and the WEHI FACS facility for expert assistance.

Funding

K.D.S is supported by the Peter and Julie Alston Centenary Fellowship; M.E.R is a recipient of an NHMRC Career Development Fellowship (GNT1104924); C. A-C is the recipient of an Australian Lung Foundation Ph.D. Scholarship; S.D and M.E.V are supported by an NHMRC project grant (APP1063837) and an ARC DECRA grant (DE140100500), M-L A-L is supported by a Viertel Foundation Senior Medical Research Fellowship; S.A.B. is supported by a Victorian Cancer Agency (VCA) Early Career Seed Grant (ECSG16001). This work was made possible through Victorian State Government Operational Infrastructure Support and Australian Government.

Data availability

The complete RNA-seq dataset is available at Gene Expression Omnibus with accession number GSE105781.

Conflict of interest

The authors declare no potential conflicts of interest

Appendix A. Supporting information

Supplementary data associated with this article can be found in the online version at doi:10.1016/j.ydbio.2018.09.002.

References

Alanis, D.M., Chang, D.R., Akiyama, H., Krasnow, M.A., Chen, J., 2014. Two nested developmental waves demarcate a compartment boundary in the mouse lung. Nat.

Commun. 5, 3923.
Auden, A., Caddy, J., Wilanowski, T., Ting, S.B., Cunningham, J.M., Jane, S.M., 2006. Spatial and temporal expression of the Grainyhead-like transcription factor family during murine development.. Gene Expr. Patterns: GEP 6, 964–970.
Aue, A., Hinze, C., Walentin, K., Ruffert, J., Yurtdas, Y., Werth, M., Chen, W., Rabien, A., Kilic, E., Schulzke, J.D., Schumann, M., Schmidt-Ott, K.M., 2015. A Grainyhead-like 2/Ovo-like 2 pathway regulates renal epithelial barrier function and lumen expansion. J. Am. Soc. Nephrol.: JASN 26, 2704–2715.
Barker, H.E., Smyth, G.K., Wettenhall, J., Ward, T.A., Bath, M.L., Lindeman, G.J., Visvader, J.E., 2008. Deaf-1 regulates epithelial cell proliferation and side-branching in the mammary gland. BMC Dev. Biol. 8, 94.
Bilodeau, M., Shojaie, S., Ackerley, C., Post, M., Rossant, J., 2014. Identification of a proximal progenitor population from murine fetal lungs with clonogenic and multilineage differentiation potential. Stem Cell Rep. 3, 634–649.
Caddy, J., Wilanowski, T., Darido, C., Dworkin, S., Ting, S.B., Zhao, Q., Rank, G., Auden, A., Srivastava, S., Papenfuss, T.A., Murdoch, J.N., Humbert, P.O., Parekh, V., Boulos, N., Weber, T., Zuo, J., Cunningham, J.M., Jane, S.M., 2010. Epidermal wound repair is regulated by the planar cell polarity signaling pathway. Dev. Cell 19, 138–147.
Desai, T.J., Brownfield, D.G., Krasnow, M.A., 2014. Alveolar progenitor and stem cells in lung development, renewal and cancer. Nature 507, 190–194.
Dompe, N., Rivers, C.S., Li, L., Cordes, S., Schwickart, M., Punnoose, E.A., Amler, L., Seshagiri, S., Tang, J., Modrusan, Z., Davis, D.P., 2011. A whole-genome RNAi screen identifies an 8q22 gene cluster that inhibits death receptor-mediated apoptosis. Proc. Natl. Acad. Sci. USA 108, E943–E951.
Dworkin, S., Darido, C., Georgy, S.R., Wilanowski, T., Srivastava, S., Ellett, F., Pase, L., Han, Y., Meng, A., Heath, J.K., Lieschke, G.J., Jane, S.M., 2012. Midbrain-hindbrain boundary patterning and morphogenesis are regulated by diverse grainy head-like 2-dependent pathways. Development 139, 525–536.
Dworkin, S., Simkin, J., Darido, C., Partridge, D.D., Georgy, S.R., Caddy, J., Wilanowski, T., Lieschke, G.J., Doggett, K., Heath, J.K., Jane, S.M., 2014. Grainyhead-like 3 regulation of endothelin-1 in the pharyngeal endoderm is critical for growth and development of the craniofacial skeleton. Mech. Dev. 133, 77–90.
Galvis, L.A., Holik, A.Z., Short, K.M., Pasquet, J., Lun, A.T., Blewitt, M.E., Smyth, I.M., Ritchie, M.E., Asselin-Labat, M.L., 2015. Repression of Igf1 expression by Ezh2 prevents basal cell differentiation in the developing lung. Development 142, 1458–1469.
Gao, X., Bali, A.S., Randell, S.H., Hogan, B.L., 2015. GRHL2 coordinates regeneration of a polarized mucociliary epithelium from basal stem cells. J. Cell Biol. 211, 669–682.
Gao, X., Vockley, C.M., Pauli, F., Newberry, K.M., Xue, Y., Randell, S.H., Reddy, T.E., Hogan, B.L., 2013. Evidence for multiple roles for grainyhead-like 2 in the establishment and maintenance of human mucociliary airway epithelium. Proc. Natl. Acad. Sci. USA 110, 9356–9361.
Gontan, C., de Munck, A., Vermeij, M., Grosveld, F., Tibboel, D., Rottier, R., 2008. Sox2 is important for two crucial processes in lung development: branching morphogenesis and epithelial cell differentiation. Dev. Biol. 317, 296–309.
Grant, C.E., Bailey, T.L., Noble, W.S., 2011. FIMO: scanning for occurrences of a given motif. Bioinformatics 27, 1017–1018.
Guseh, J.S., Bores, S.A., Stanger, B.Z., Zhou, Q., Anderson, W.J., Melton, D.A., Rajagopal, J., 2009. Notch signaling promotes airway mucous metaplasia and inhibits alveolar development. Development 136, 1751–1759.
Harfe, B.D., Scherz, P.J., Nissim, S., Tian, H., McMahon, A.P., Tabin, C.J., 2004. Evidence for an expansion-based temporal Shh gradient in specifying vertebrate digit identities. Cell 118, 517–528.
Hemphala, J., Uv, A., Cantera, R., Bray, S., Samakovlis, C., 2003. Grainy head controls apical membrane growth and tube elongation in response to branchless/FGF signalling. Development 130, 249–258.
Herriges, M., Morrisey, E.E., 2014. Lung development: orchestrating the generation and regeneration of a complex organ. Development 141, 502–513.
Jolma, A., Yan, J., Whitington, T., Toivonen, J., Nitta, K.R., Rastas, P., Morgunova, E., Enge, M., Taipale, M., Wei, G., Palin, K., Vaquerizas, J.M., Vincentelli, R., Luscombe, N.M., Hughes, T.R., Lemaire, P., Ukkonen, E., Kivioja, T., Taipale, J., 2013. DNA-binding specificities of human transcription factors. Cell 152, 327–339.
Kage, H., Flodby, P., Gao, D., Kim, Y.H., Marconett, C.N., DeMaio, L., Kim, K.J., Crandall, E.D., Borok, Z., 2014. Claudin 4 knockout mice: normal physiological phenotype with increased susceptibility to lung injury. Am. J. Physiol. Lung Cell. Mol. Physiol. 307, L524–L536.
Kinsella, J.P., Greenough, A., Abman, S.H., 2006. Bronchopulmonary dysplasia. Lancet 367, 1421–1431.
Liao, Y., Smyth, G.K., Shi, W., 2013. The Subread aligner: fast, accurate and scalable read mapping by seed-and-vote. Nucleic Acids Res. 41, e108.
Liao, Y., Smyth, G.K., Shi, W., 2014. featureCounts: an efficient general purpose program for assigning sequence reads to genomic features. Bioinformatics 30, 923–930.
Liu, R., Holik, A.Z., Su, S., Jansz, N., Chen, K., Leong, H.S., Blewitt, M.E., Asselin-Labat, M.L., Smyth, G.K., Ritchie, M.E., 2015. Why weight? Modelling sample and observational level variability improves power in RNA-seq analyses. Nucleic Acids Res. 43, e97.
Merino, D., Best, S.A., Asselin-Labat, M.L., Vaillant, F., Pal, B., Dickins, R.A., Anderson, R.L., Strasser, A., Bouillet, P., Lindeman, G.J., Visvader, J.E., 2015. Pro-apoptotic bim suppresses breast tumor cell metastasis and is a target gene of SNAI2. Oncogene 34, 3926–3934.
Metzger, D.E., Stahlman, M.T., Shannon, J.M., 2008. Misexpression of ELF5 disrupts lung branching and inhibits epithelial differentiation. Dev. Biol. 320, 149–160.
Metzger, D.E., Xu, Y., Shannon, J.M., 2007. Elf5 is an epithelium-specific, fibroblast growth factor-sensitive transcription factor in the embryonic lung. Dev. Dyn. 236, 1175–1192.
Morrisey, E.E., Hogan, B.L., 2010. Preparing for the first breath: genetic and cellular mechanisms in lung development. Dev. Cell 18, 8–23.
Nikolic, M.Z., Caritg, O., Jeng, Q., Johnson, J.A., Sun, D., Howell, K.J., Brady, J.L., Laresgoiti, U., Allen, G., Butler, R., Zilbauer, M., Giangreco, A., Rawlins, E.L., 2017. Human embryonic lung epithelial tips are multipotent progenitors that can be expanded in vitro as long-term self-renewing organoids. eLife 6.
Oakes, S.R., Naylor, M.J., Asselin-Labat, M.L., Blazek, K.D., Gardiner-Garden, M., Hilton, H.N., Kazlauskas, M., Pritchard, M.A., Chodosh, L.A., Pfeffer, P.L., Lindeman, G.J., Visvader, J.E., Ormandy, C.J., 2008. The Ets transcription factor Elf5 specifies mammary alveolar cell fate. Genes Dev. 22, 581–586.
Oettgen, P., Kas, K., Dube, A., Gu, X., Grall, F., Thamrongsak, U., Akbarali, Y., Finger, E., Boltax, J., Endress, G., Munger, K., Kunsch, C., Libermann, T.A., 1999. Characterization of ESE-2, a novel ESE-1-related Ets transcription factor that is restricted to glandular epithelium and differentiated keratinocytes. J. Biol. Chem. 274, 29439–29452.
Pan, X., Zhang, R., Xie, C., Gan, M., Yao, S., Yao, Y., Jin, J., Han, T., Huang, Y., Gong, Y., Wang, J., Yu, B., 2017. GRHL2 suppresses tumor metastasis via regulation of transcriptional activity of RhoG in non-small cell lung cancer. Am. J. Transl. Res 9, 4217–4226.
Petrof, G., Nanda, A., Howden, J., Takeichi, T., McMillan, J.R., Aristodemou, S., Ozoemena, L., Liu, L., South, A.P., Pourreyron, C., Dafou, D., Proudfoot, L.E., Al-Ajmi, H., Akiyama, M., McLean, W.H., Simpson, M.A., Parsons, M., McGrath, J.A., 2014. Mutations in GRHL2 result in an autosomal-recessive ectodermal Dysplasia syndrome. Am. J. Hum. Genet. 95, 308–314.
Pyrgaki, C., Liu, A., Niswander, L., 2011. Grainyhead-like 2 regulates neural tube closure and adhesion molecule expression during neural fold fusion. Dev. Biol. 353, 38–49.
Que, J., Luo, X., Schwartz, R.J., Hogan, B.L., 2009. Multiple roles for Sox2 in the developing and adult mouse trachea. Development 136, 1899–1907.
Rawlins, E.L., Clark, C.P., Xue, Y., Hogan, B.L., 2009. The Id2+ distal tip lung epithelium contains individual multipotent embryonic progenitor cells. Development 136, 3741–3745.
Rifat, Y., Parekh, V., Wilanowski, T., Hislop, N.R., Auden, A., Ting, S.B., Cunningham, J.M., Jane, S.M., 2010. Regional neural tube closure defined by the Grainy head-like transcription factors. Dev. Biol. 345, 237–245.
Ritchie, M.E., Phipson, B., Wu, D., Hu, Y., Law, C.W., Shi, W., Smyth, G.K., 2015. limma powers differential expression analyses for RNA-sequencing and microarray studies. Nucleic Acids Res. 43, e47.
Robinson, M.D., McCarthy, D.J., Smyth, G.K., 2010. edgeR: a bioconductor package for differential expression analysis of digital gene expression data. Bioinformatics 26, 139–140.
Robinson, M.D., Oshlack, A., 2010. A scaling normalization method for differential expression analysis of RNA-seq data. Genome Biol. 11, R25.
Rockich, B.E., Hrycaj, S.M., Shih, H.P., Nagy, M.S., Ferguson, M.A., Kopp, J.L., Sander, M., Wellik, D.M., Spence, J.R., 2013. Sox9 plays multiple roles in the lung epithelium during branching morphogenesis. Proc. Natl. Acad. Sci. USA 110, E4456–E4464.
Schindelin, J., Arganda-Carreras, I., Frise, E., Kaynig, V., Longair, M., Pietzsch, T., Preibisch, S., Rueden, C., Saalfeld, S., Schmid, B., Tinevez, J.Y., White, D.J., Hartenstein, V., Eliceiri, K., Tomancak, P., Cardona, A., 2012. Fiji: an open-source platform for biological-image analysis. Nat. Methods 9, 676–682.
Schwenk, F., Baron, U., Rajewsky, K., 1995. A cre-transgenic mouse strain for the ubiquitous deletion of loxP-flanked gene segments including deletion in germ cells. Nucleic Acids Res. 23, 5080–5081.
Short, K., Hodson, M., Smyth, I., 2013. Spatial mapping and quantification of developmental branching morphogenesis. Development 140, 471–478.
Ting, S.B., Caddy, J., Hislop, N., Wilanowski, T., Auden, A., Zhao, L.L., Ellis, S., Kaur, P., Uchida, Y., Holleran, W.M., Elias, P.M., Cunningham, J.M., Jane, S.M., 2005. A homolog of Drosophila grainy head is essential for epidermal integrity in mice. Science 308, 411–413.
Ting, S.B., Wilanowski, T., Auden, A., Hall, M., Voss, A.K., Thomas, T., Parekh, V., Cunningham, J.M., Jane, S.M., 2003. Inositol- and folate-resistant neural tube defects in mice lacking the epithelial-specific factor Grhl-3. Nat. Med. 9, 1513–1519.
Tompkins, D.H., Besnard, V., Lange, A.W., Keiser, A.R., Wert, S.E., Bruno, M.D., Whitsett, J.A., 2011. Sox2 activates cell proliferation and differentiation in the respiratory epithelium. Am. J. Respir. Cell Mol. Biol. 45, 101–110.
Treutlein, B., Brownfield, D.G., Wu, A.R., Neff, N.F., Mantalas, G.L., Espinoza, F.H., Desai, T.J., Krasnow, M.A., Quake, S.R., 2014. Reconstructing lineage hierarchies of the distal lung epithelium using single-cell RNA-seq. Nature 509, 371–375.
Tsao, P.N., Vasconcelos, M., Izvolsky, K.I., Qian, J., Lu, J., Cardoso, W.V., 2009. Notch signaling controls the balance of ciliated and secretory cell fates in developing airways. Development 136, 2297–2307.
Varma, S., Mahavadi, P., Sasikumar, S., Cushing, L., Hyland, T., Rosser, A.E., Riccardi, D., Lu, J., Kalin, T.V., Kalinichenko, V.V., Guenther, A., Ramirez, M.I., Pardo, A., Selman, M., Warburton, D., 2014. Grainyhead-like 2 (GRHL2) distribution reveals novel pathophysiological differences between human idiopathic pulmonary fibrosis and mouse models of pulmonary fibrosis. Am. J. Physiol. Lung Cell. Mol. Physiol. 306, L405–L419.
Voss, A.K., Dixon, M.P., McLennan, T., Kueh, A.J., Thomas, T., 2012. Chromatin immunoprecipitation of mouse embryos. Methods Mol. Biol. 809, 335–352.
Walentin, K., Hinze, C., Werth, M., Haase, N., Varma, S., Morell, R., Aue, A., Potschke, E., Warburton, D., Qiu, A., Barasch, J., Purfurst, B., Dieterich, C., Popova, E., Bader, M., Dechend, R., Staff, A.C., Yurtdas, Z.Y., Kilic, E., Schmidt-Ott, K.M., 2015. A Grhl2-dependent gene network controls trophoblast branching morphogenesis. Development 142, 1125–1136.
Wang, H., St Julien, K.R., Stevenson, D.K., Hoffmann, T.J., Witte, J.S., Lazzeroni, L.C., Krasnow, M.A., Quaintance, C.C., Oehlert, J.W., Jelliffe-Pawlowski, L.L., Gould, J.B., Shaw, G.M., O'Brodovich, H.M., 2013. A genome-wide association study (GWAS) for bronchopulmonary dysplasia. Pediatrics 132, 290–297.

Warburton, D., Schwarz, M., Tefft, D., Flores-Delgado, G., Anderson, K.D., Cardoso, W.V., 2000. The molecular basis of lung morphogenesis. Mech. Dev. 92, 55–81.
Warburton, D., Seth, R., Shum, L., Horcher, P.G., Hall, F.L., Werb, Z., Slavkin, H.C., 1992. Epigenetic role of epidermal growth factor expression and signalling in embryonic mouse lung morphogenesis. Dev. Biol. 149, 123–133.
Werth, M., Walentin, K., Aue, A., Schonheit, J., Wuebken, A., Pode-Shakked, N., Vilianovitch, L., Erdmann, B., Dekel, B., Bader, M., Barasch, J., Rosenbauer, F., Luft, F.C., Schmidt-Ott, K.M., 2010. The transcription factor grainyhead-like 2 regulates the molecular composition of the epithelial apical junctional complex. Development 137, 3835–3845.
Wu, D., Lim, E., Vaillant, F., Asselin-Labat, M.L., Visvader, J.E., Smyth, G.K., 2010. ROAST: rotation gene set tests for complex microarray experiments. Bioinformatics 26, 2176–2182.
Young, M.D., Wakefield, M.J., Smyth, G.K., Oshlack, A., 2010. Gene ontology analysis for RNA-seq: accounting for selection bias. Genome Biol. 11, R14.
Zhou, J., Ng, A.Y., Tymms, M.J., Jermiin, L.S., Seth, A.K., Thomas, R.S., Kola, I., 1998. A novel transcription factor, ELF5, belongs to the ELF subfamily of ETS genes and maps to human chromosome 11p13-15, a region subject to LOH and rearrangement in human carcinoma cell lines. Oncogene 17, 2719–2732.
Zhu, L.J., Gazin, C., Lawson, N.D., Pages, H., Lin, S.M., Lapointe, D.S., Green, M.R., 2010. ChIPpeakAnno: a Bioconductor package to annotate ChIP-seq and ChIP-chip data. BMC Bioinforma. 11, 237.